Shock Waves (1991) 1:51–63

Shock Waves

Color schlieren methods in shock wave research

H. Kleine and H. Grönig

Stosswellenlabor RWTH, Templergraben 55, D-5100 Aachen, Federal Republic of Germany

Received August 24, 1990; accepted September 25, 1990

Abstract. Schlieren methods are widely known and well established to visualize refractive index variations in transparent media. The use of color allows one to obtain more data and previously inaccessible information from a picture taken with this technique. In general, a hue can be related to a certain strength or a certain direction of a refractive index gradient. While the first case essentially corresponds to the usual black-and-white system the latter correlation cannot be made adequately evident without the use of color. Two color schlieren techniques are presented here, which reach or even exceed the quality and sensitivity range of conventional black-and-white methods. Using a powerful short duration light source these methods are applied to visualize transient flow phenomena in a shock tube.

Key words: Flow visualization, Color schlieren, Shock wave interaction

1. Introduction

Color schlieren methods have been known almost since the invention and first application of the schlieren technique. While color shifts due to chromatic aberrations of the optical components of the apparatus have been observed (and mostly cursed) since the early beginnings, a first attempt to employ color intentionally was made in 1896 by Rheinberg. Since then a vast variety of methods have been developed for various applications. A comprehensive overview is given by Settles (1982); his survey provides the basis for the brief historical review given here. Although most authors claim to have reached satisfying results for their special purposes, color methods still have the aura of being exotic and mostly ostentatious techniques with only little scientific usefulness. Moreover, higher demands on the optical components of the setup as well as the additional complexity concerning processing and reproduction of color pictures have kept many people from employing these methods. Although it is not the purpose of this paper to take part in a general discussion on the utility of color in schlieren applications, the authors believe that the diagnostic potential inherent in these methods has been widely overlooked and neglected so far: color systems can be made equivalent or even superior to traditional black-and-white techniques. There will, however, be a large number of cases where black-and-white pictures may be fully sufficient or even more useful, but there are also many examples where one is enabled to interpret certain phenomena only with the help of color. As it will be shown this is particularly true for the analysis of rather complex flow structures where monochrome pictures might be unclear and puzzling rather than informative.

It should be stated beforehand that for the short duration application at least the one-dimensional type color system only can reach or exceed the *sensitivity range* of a corresponding black-and-white apparatus but not the *maximum sensitivity* itself. In other words, black-and-white systems can be made more sensitive, but then they will 'overshoot' more quickly than the color version in the case of stronger gradients. In setups where the effective output of a light source can be arbitrarily magnified (which from a certain level on will mainly be done by increasing the exposure time) color systems may yield a maximum sensitivity close to the value given by black-and-white configurations.

2. Optical principle

As the schlieren principle is both well understood and well commented and reviewed (Schardin 1942; Holder and North 1956; Oertel and Oertel 1989), only a brief outline will follow now to clarify both potential and limitations of that technique.

Schlieren methods applied in flow visualization are based on the fact that the refractive index of a transpar-

Offprint requests to: H. Grönig

ent fluid depends on the fluid state. For a given medium and a particular wavelength of the transmitted light, the refractive index will only depend on the density of the medium. In gases this relationship can be expressed as a linear function. A light beam traversing a medium with local changes of density (and thus refractive index) will be refracted towards the region of increased density, with the amount of refraction being proportional to the density gradient perpendicular to the optical path. Flows with sufficiently high changes of properties will thus influence a traversing light beam. By separating the refracted part of the light, one can form an image of the disturbance responsible for the change of refractive index.

In a typical setup like the one sketched in Fig. 1 this separation is carried out in the so-called source image or cutoff plane: light that has been deflected by some disturbance in the test section is intercepted here at the schlieren stop (which is a knife edge in black-and-white applications) before it can reach the camera. Consequently, if there is a refractive index change at some point in the test section, in a monochrome system that particular point will appear brighter or darker on the film depending on strength and sign of the encountered gradient.

The use of color requires some changes as far as light source and/or cutoff device are concerned. In any case, a simple knife edge will no longer be sufficient . In fact, the need for a more complex cutoff device poses one of the major problems of color schlieren methods. More or less minor modifications of the setup employ slits or filter arrangements in the cutoff plane to code a certain light deflection. If the knife edge is simply replaced by a set of filters with the rest of the system unaltered (Rheinberg 1896; Schardin 1942; North 1954), then the sensitivity of the apparatus obviously depends on the width of the filter segments. Similarly, the width of a slit determines the performance of the configuration in the case of the prism method (Schardin 1942; Holder and North 1952). So, in principle, an enhanced sensitivity can be achieved by reducing the size of the slit or the filter segments, respectively. Actually, the possible width of slits or filter strips is severely limited due to diffraction effects, which drastically degrade the image quality. Rather large values are needed as indicated by an expression experimentally derived by Cords (1968):

$$b = \frac{0.65\lambda U}{d} \qquad (1)$$

where λ is the wavelength of light, U is the distance between test section and schlieren mirror, d is the size of the smallest object to be resolved and b is the slit width in the cutoff plane.

In our case, for $U = 2800$ mm and $d = 0.2$ mm with $\lambda = 600$ nm it follows that $b = 5.5$ mm. Any gain in sensitivity by remaining below this value causes a loss in image resolution and quality. In fact, sensitivity cannot really be enhanced that way, since, in a diffraction-degraded image, small disturbances simply cannot be resolved any more although they might have caused a color shift. Things are even worse in the case of filter strip arrangements in the cutoff plane due to diffraction caused by the filter edges and / or impurities on the filters such as scratches or cuts. Some improvement can be made by replacing the filter strips with a color wedge filter, where at least the influence of the edges can be eliminated.

With these limitations, color methods of that kind only seemed to be applicable in cases where strong gradients were to be visualized. In most examples the inevitable shortcomings of these methods were partially veiled by employing schlieren mirrors of very large focal length thus gaining some sensitivity and reaching acceptable results. Still, the principle drawback was not solved until 1968, when Cords introduced the dissection technique: the separation into different colors is carried out by a colored filter mask in the source plane; several colored bands are placed there with a spacing of a few millimeters. The corresponding cutoff device is a slit whose width matches the distance of the inner color bands. As both distance and color combination can be chosen rather arbitrarily, diffraction effects can be avoided and a variety of color spectra for coding the gradients can be obtained. Moreover, small defects of the filters have no significant image-degrading influence. An adequate sensitivity can be attained by narrowing the colored segments.

In the methods described so far the *strength* of the encountered gradient is related to a certain color or a corresponding shade of gray. An unambiguous relation can only be achieved in one direction, consequently only one component of a usually quasi-two-dimensional flow field can be visualized in one picture. These methods therefore are said to work one-dimensionally. Introducing color offers an additional dimension: Rheinberg (1896), Wolter (1950) and Wuest (1967) had already recognized the possibility of coding the *direction* of a gradient with a certain color, but their approaches suffered from the above mentioned losses either in sensitivity or resolution. Settles (1970) was the first to combine the ideas of a direction indicating system with Cords' dissection technique. His method was used in a number of fine applications (Stong 1971; Vandiver and Edgerton 1974), although the overall response to that technique was not exactly overwhelming. A proposed simplification of the method (Settles 1982) followed, but again had only a few utilizations (Settles 1983; Settles and Kuhns 1984; Hibberd 1986). To the best of the authors' knowledge, apart from some visualizations in the field of ballistics and hypersonics (Settles 1985) practically no successful application of that method has been realized so far for visualizing transient shock wave related phenomena, especially for the detailed study of shock systems emerging from the interaction of shock waves with obstacles or area changes.

When correlating a color and a gradient direction, the obtained picture simultaneously records all density gradients normal to the optical path encountered in the flow field at the moment the image is taken. Thus, fully two-dimensional information about the flow field

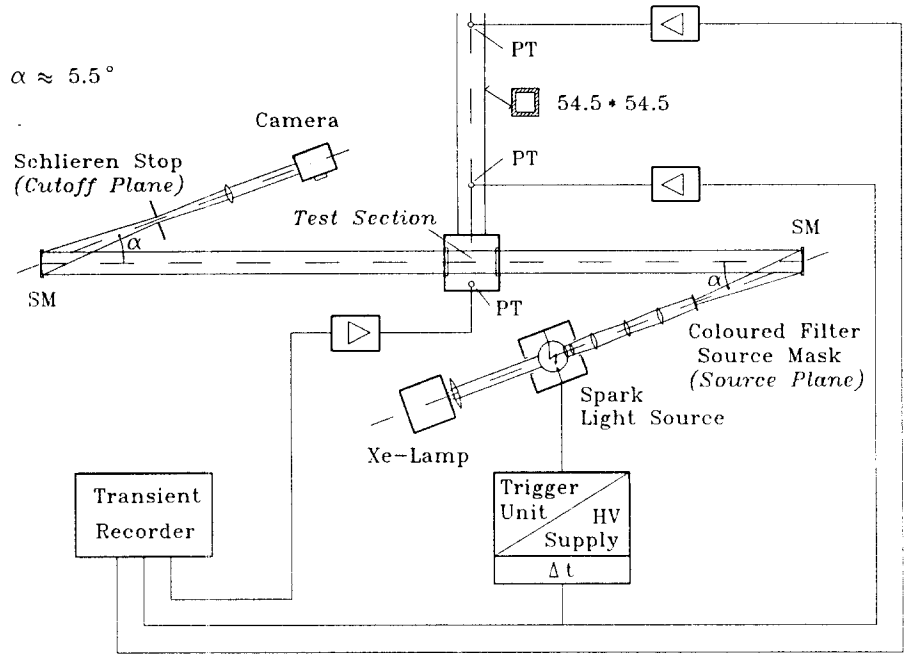

Fig. 1. Schematic sketch of experimental setup. SM: Spherical Mirror (f = 2000mm), PT: Pressure Transducer

is contained in a single picture. However, it is difficult now to determine the strength of the gradients, as color saturation - being roughly the equivalent to the shades of gray in black-and white - is hard to estimate.

3. Experimental setup

The setup used here corresponds to the classic Toepler-Z-configuration-with two exceptions (see Fig. 1): in a usual black-and-white configuration the lens system behind the spark light source creates an image of the spark in the source plane (the focal plane of the first spherical mirror), while in this setup the lenses are adjusted in a way to make the light of the spark uniformly illuminate a colored filter source mask situated in that source plane. This is equivalent to forming a set of approximate point light sources each of which will produce a parallel light beam in its own color. The individual beams mix to form the parallel light beam traversing the test section. Separation into the components is carried out by the second spherical mirror, which refocusses the collimated beam creating an inverted, same-size image of the source mask in its focal plane (focal length of both spherical mirrors: 2000 mm). Depending on the selected mask, either a slit (consisting of two knife edges) or a cylindrical pinhole (or more conveniently, an iris diaphragm) serves as the schlieren stop cutting off all beams but one. The light that is thus admitted to the film without any refraction in the test section produces the background color. Any change of refractive index along the optical path leads to a displacement of the images of the colored sectors at the schlieren stop causing other colors to appear on the film. Mixing of colors will yield yellow, blue-green and violet in different shades next to the basic colors red, blue and green. In the case of the one-dimensional method, other hues like a bluish white or a light blue-gray also appear by corresponding color combinations.

The light source for the color pictures is a Xe-filled flashlamp designed by Ciezki (1984) and previously used by Hermann (1987) for the development of another one-dimensional color schlieren method. With a spark duration of about 1200 ns FWHM[1] the light output is sufficiently high to expose customary ASA 400 slide film. In some cases, however, an uncontrolled spark afterglow has been recorded: some additional light (in magnitude about 10% of the peak value) is emitted for another 3 to 5μs thus creating a 'long-time' schlieren effect. Flow patterns that don't change significantly during that period (such as slip lines or certain reflected waves) are thus also visualized by this subsequent exposure of the film. The faint lines preceding the shock front in Fig. 5b result from such a 'long-time' visualization. With further knowledge of the process these lines can be identified as a set of slowly moving slip lines created by the leading shock system. A similar phenomenon was observed by Ben-Dor et al. (1986), but was interpreted differently at that time.

For the black-and-white pictures shown here, the light source with subsequent lens system and cutoff device are replaced by equivalent components used for a conventional black-and-white setup, while the general layout of the system remains unchanged. The light source employed in that configuration is an enlarged version of the source NANOSPARK developed by Miyashiro and Grönig (1984). Although spark duration (≈ 60 ns

[1] FWHM: full width half maximum designates the half width of a pulse and is used as a standard definition of pulse duration

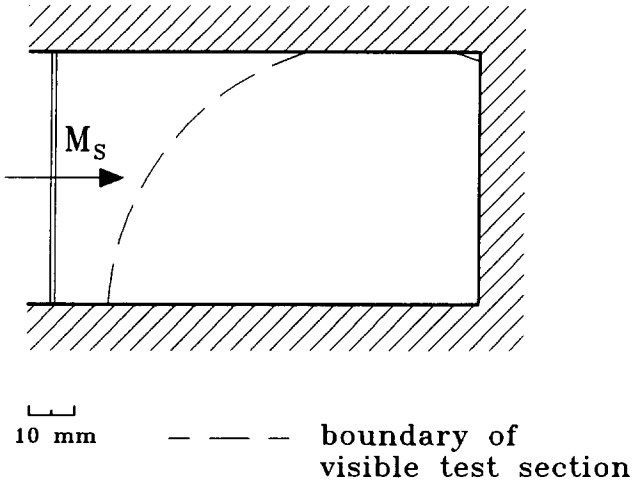

Fig. 2. Test section

FWHM) and light intensity are significantly smaller than for the Xe-flashlamp, standard ASA 100 film can be exposed quite well, as black-and- white systems use the offered light much more efficiently than color configurations.

The shock tube used in these experiments (total length 9400 mm, length of low pressure part 6200 mm) has a square cross section of 54.5 mm × 54.5 mm, the test section being located at the end of the low pressure part. The basic test section type for the examples presented here is shown in Fig. 2. According to the problem to be investigated its shape can be changed by various replaceable inserts. The asymmetric position of the test section windows that leads to the quarter-circle shape of the pictures is caused by the requirement to visualize both the flow in the main channel as well as in subsequent branching off ducts. The shock Mach number M_s given with the pictures of Figs. 5-8 is obtained by a pressure / time measurement at the end of the low pressure part (accuracy : ±0.01).

Fig. 8c was taken at the Aachen shock tunnel (for a description of this facility see Olivier and Grönig 1988) with an almost identical optical system. Here M_∞ and Re_∞ are the free stream Mach number and free stream Reynolds number per meter, respectively.

4. Color schlieren methods

The crucial element of an apparatus employing the ideas of the dissection technique is the colored filter source mask. As already proposed by several authors the masks can be easily manufactured photographically using a high contrast black-and-white film. The pattern of the mask is drawn in black and white and photographed afterwards in the desired scale. The negative obtained that way serves as the basis of the mask. Gelatine filter strips are placed behind the transparent parts and are then fixed with some glue or adhesive tape. From the manufacturer's point of view, the only limitation in choosing the geometry of the mask is the need for some space in between the segments to allow fixing of the filter strips. Remaining dark parts of the mask may be made completely opaque by means of some additional shielding, although this is not necessary if the film is adequately exposed. Once the mask has been assembled this way, a diffusing screen is placed immediately behind it. This unit now serves as the colored filter source mask, which is placed in the focal plane of the first spherical mirror.

The performance of the apparatus can easily be calibrated and made visible by inserting an object of known refractive index distribution into the test section. As already suggested by Schardin (1942), a plano-convex lens with a large focal length is a suitable calibration device. This lens causes a deflection of the light beam of

$$\gamma \approx tan\gamma = \frac{y_L}{f} \tag{2}$$

where y_L is the distance from the center of the lens ($0 \leq y_L \leq$ lens radius) and f is the focal length of the calibration lens.

Equating this with the angular deflection of a light beam for a two-dimensional flow

$$\varepsilon = \frac{L}{n_0}\frac{\partial n}{\partial x}\bigg|_P \tag{3}$$

where L is the width of the test section, n_0 is the refractive index of the air surrounding the test section, n is the refractive index at a given point P in the test section and x is a coordinate perpendicular to both the optical path and the edges of the cutoff device, and using the refractive index / density relation for gases leads to

$$\frac{\partial \rho}{\partial x}\bigg|_P = \frac{y_L}{LKf}(1 + K\rho_0) \approx \frac{y_L}{LKf} \tag{4}$$

where ρ is the density at a given point P in the test section and K is the Gladstone-Dale constant of the test gas. x and y_L have to be equidirectional coordinates if (4) is to be valid.

The latter approximation is equivalent to the assumption that $n_0 \approx 1$. Thus, by taking a picture with the inserted calibration lens, both dynamic range and sensitivity of the system are determined. For the one-dimensional method, the correlation between strength of a gradient (with respect to the chosen direction) and a color is easily obtained and a rough quantitative analysis of the picture can be made without the help of photometric devices, see Figs. 5c, 6c, 7c. In the case of the two-dimensional technique, the picture of the lens yields the color / gradient direction correlation similar to a polar diagram, see Figs. 3b and 5b. Here, the change of color along a line of constant angle is hardly perceptible, so that any conclusion concerning the strength of the gradient is at least very doubtful.

The calibration lens used in these experiments had a focal length of 10 m and a diameter of 29 mm. For the one-dimensional method, (4) yields that one millimeter

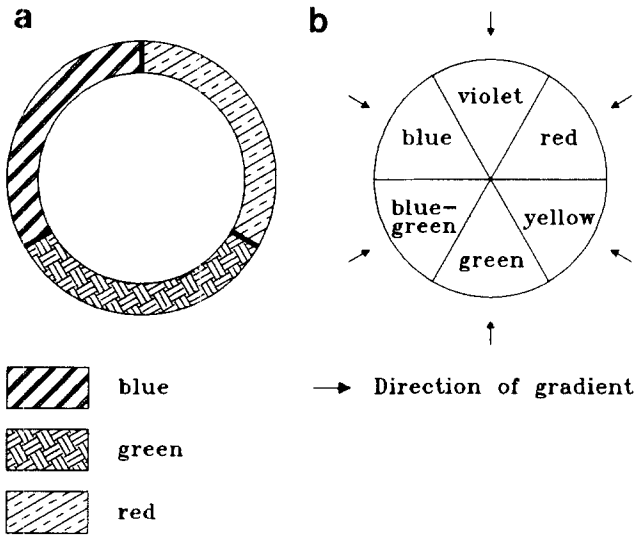

Fig. 3. a Colored filter source mask (2-D method), b correlation between gradient direction and image color

of y_L corresponds to a density gradient in air of roughly 7 kg/m^4, the maximum total gradient range covered by the lens being -100 kg/m^4 to +100 kg/m^4. In the calibration pictures of Figs. 5c, 6c and 7c, the colors left of the neutral state background color represent increasing density gradients with respect to the flow direction, hues right of the center color correspondingly code expansion zones.

5. Two-dimensional color schlieren method

The technique applied here is based on the proposal by Settles (1982). For the colored filter source mask of Fig. 3a colors and gradient directions are correlated as indicated in Fig. 3b. Due to the above mentioned diffraction effects, the inner diameter of the mask should not be smaller than about 6 mm, while the width of the colored bands may vary from 0.25 mm to 1.5 mm. Very small values of the width cause an early overshooting (for example, the center of the vortex of Fig. 8a would have been opaque if the mask had had thinner bands), while broad bands lead to a desaturation of colors in the picture.

The need for some background color also calls for a comparatively large value of the inner diameter of the mask. The background color is obtained by allowing a portion of one band to pass the schlieren stop in the absence of any gradient in the test section. Without that background, all impurities such as scratches or dust particles on the test section windows (simply anything that causes light scattering) would become visible as tiny bright spots or lines. In addition, without a background color the pictures would become intolerably dark. For these reasons, the iris diaphragm in the cutoff plane is shifted by a small distance thus admitting one color (or the mixture of two) onto the film. The center of the correlation diagram of Fig. 3b is then correspondingly displaced in the opposite direction. In order to maintain the symmetry at least to some extent, the displacement of the schlieren stop must be as small as possible. On the other hand, the total amount of light thus reaching the film must be enough for a sufficient flooding of the background. Combining these two demands leads to a comparatively large inner diameter of the mask.

By moving the schlieren stop vertically or horizontally, any color can be chosen for the background. In this case the relationship of Fig. 3b does not change, only the center point is shifted slightly as already mentioned. Another background color will come up as well if the mask is rotated without moving the schlieren stop. Then, of course, the polar diagram of Fig. 3b is rotated likewise. If it is not planned to play around with the background color, enlarging one of the segments helps to keep the mask diameter down to smaller values, and allows central alignment of the iris diaphragm. However, as the asymmetry of the corresponding sector in the correlation diagram is retained, no major improvements can be achieved this way.

For most of our applications, a green background proved to yield the highest contrast and thus the most impressive pictures. For all presented examples of the two-dimensional method, except Fig. 8c, the color/gradient direction correlation of Fig. 3b or Fig. 5b, respectively, is valid. The correlation diagram for Fig. 8c is the inverse of Fig. 3b - each sector has to be replaced by its corresponding opposite one.

Considering the shapes of mask and cutoff device it is obvious that any color can be formed almost immediately even by small deflections. Thus, the two-dimensional technique exhibits a sensitivity comparable to that of black-and-white systems. This has also been proved by a successful application of this method concerning the visualization of hypersonic flows, where the initial densities are markedly lower than in a conventional shock tube (Fig. 8c).

As this method yields fully two-dimensional refractive index information, it is obviously suitable for visualizing directionally dependent phenomena. Vortices, for instance, will always be recognized by a color pattern which basically is the inverse of the correlation diagram. In this way, the method allows one to detect the presence of vortices in flow fields of almost arbitrary complexity. Likewise, the determination of the onset of Mach reflection is possible: the emerging Mach stem launches a new gradient direction in the flow field thus producing a new color (Kleine et al. 1990).

The described method can be inverted by replacing the iris diaphragm in the cutoff plane by a circular plate of a size matching the outer diameter of the source mask. If in the previous setup a gradient caused, for example, a shift to red color, the same gradient would now appear in blue-green. Now, the background is almost black or at least very dark, because only refracted light reaches the film. As a result of this, the above mentioned impurities on the test section windows become more clearly visible now. Color contrast is reduced due to the lack of a background color; the sensitivity range is more eas-

ily exceeded and thus considerably smaller than for the first method. Strong disturbances will appear as bright and almost white regions veiling most of the flow field details. Still, the pictures obtained with this technique (which is designated as *darkfield schlieren method* in accordance with corresponding black-and-white systems) impressively show the main shock structures in a flow field, see Fig. 7b. However, this version should not be applied if a flow with strong vorticity is to be visualized as vortices will cause an early 'overshooting'. For the example presented in Fig. 7b, the mask was rotated by 60° - otherwise the accompanying polar diagram would have simply been the inverse of Fig. 3b.

6. One-dimensional color schlieren method

A one-dimensional color schlieren method practically records the same quantities as a traditional black-and white system. But by coding gradient strengths with color instead of shades of gray a more clearly arranged picture can be obtained, which can also be more easily analyzed without sophisticated devices. The major problem, however, is to reach a comparable sensitivity with no losses in image quality. The method applied here is an extended and optimized version of the technique developed by Cords (1968). The aim is to code a certain field of gradients with as many colors as possible with each color representing the least possible gradient range. Applying the dissection technique allows one to create a variety of color spectra but also limits the number of possible hues: as the distance between the inner color bands, Fig. 4, is much larger than the overall width of all bands on either side of the mask, at most two pure colors can be obtained in the spectrum. Only extremely strong gradients will deflect a color band as far as beyond the second knife edge of the cutoff slit. Consequently, a color once shifted into the slit will remain there unless the gradients change their signs. So, except for the colors of the inner bands, the different hues originate from mixing of colors, which is accompanied by an increasing desaturation. As it can be seen on the calibration pictures of Figs. 5c, 6c and 7c, hues at the outer region of the calibration lens (which represent the strong gradients) approach a more or less tinted white. Still, it is possible to split up the gradient range given by the calibration lens into as many as eight different regions. A mainly uniform distribution of these sectors allows one to cover the whole range equally - small changes, however, will then be hard to detect. By varying the width of the color bands it is possible to tailor a mask so that a certain gradient range is accurately resolved by many different colors while anything exceeding that range is coded with a single hue. Figure 5c shows an example for such a tailored mask with a high resolution of comparatively small gradients close to the neutral state. On the other hand, Fig. 6c presents a more uniform partitioning of colors over the whole gradient range established by the calibration lens.

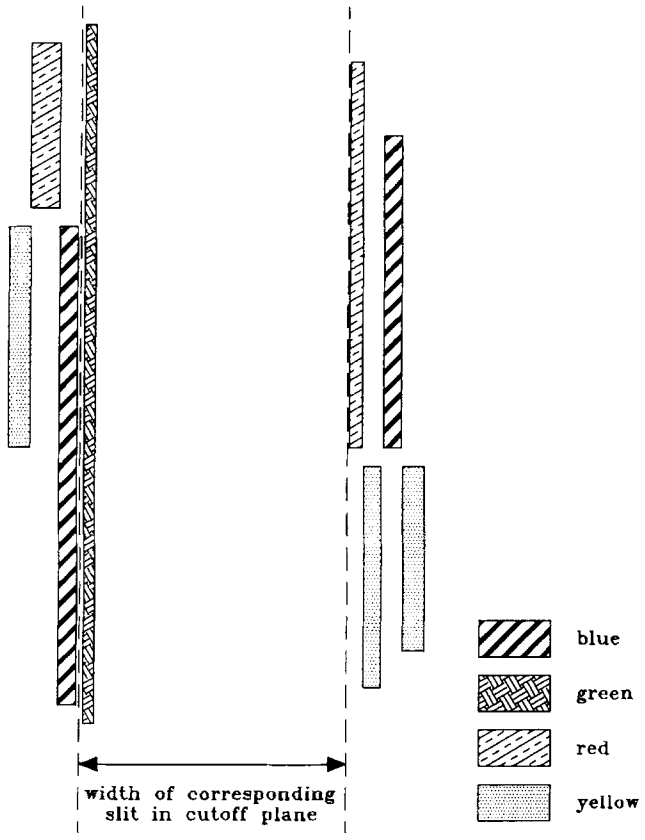

Fig. 4. Colored filter source mask (1-D method)

While the shape of the mask is more or less determined in the case of the two-dimensional method (some changes in order to tailor a mask for a certain problem are possible there as well), a larger variety of layouts may be realized in the one- dimensional case. The basic structure, of course, will always resemble the pattern proposed by Cords.

The sensitivity of the method largely depends on the width of the color bands. Again, the need for a sufficient flooding of the background calls for a minimum size of the inner band that is admitted to the film without a deflection by some gradient in the test section. Up to a certain level this value can be reached by elongating the band with the width unaltered. In principle, the width could be reduced to values below 0.1 mm thus enhancing the sensitivity. In order to get the desired background color the band then had to be several centimeters long which is both impractical and unreasonable. Very thin and yet short bands can be employed if the output of the light source can be correspondingly magnified. As this will inevitably lead to longer exposure times this possibility unfortunately has to be ruled out in short duration applications. Moreover, it should be noted that for very thin color bands diffraction effects will play an important role again. Thus, the final dimensions of the color sectors have to be chosen with respect to the desired sensitivity and the necessary amount of light to achieve both enough background color and color contrast. This

implies considering the corresponding transmission factor of the individual filters and the largest possible size of the mask. The latter value is mainly determined by the properties of the spherical mirrors or field lenses, that is, the amount of optical aberrations due to the finite size of the approximate point sources. In the setup used for the presented examples, the width of the color bands is kept above 0.25 mm still giving acceptable results which don't have to shun a comparison with black-and-white pictures. Although the dissection technique cannot provide a uniformly fine distribution of colors over a wide range of gradients, it exhibits a larger sensitivity range than a comparable monochrome method.

7. Applications

The methods described above were applied to visualize flow fields associated with the interaction of shock waves with various obstacles. As a detailed discussion of each gas dynamic problem representatively shown here might be too lengthy for this paper, only a short description will follow.

The main purpose of Figs. 5 and 6 is to show differences and similarities between the two methods and an additional comparison with a black-and-white visualization of similar high quality. As already mentioned, the black-and-white method requires less light. It will therefore be superior to the color methods as far as the image resolution is concerned, which results not only from a finer grain of the film but also from a shorter exposure time.

In Fig. 5 the interaction of a shock wave (incident shock Mach number $M_s = 1.25$ in N_2, initial pressure $p_1 = 100$ kPa) with a square section bar (edge length: 20 mm) is visualized. An increase of density in the flow direction is indicated by darker shades of gray in Fig. 5a and by the colors left of the neutral green in the calibration picture of Fig. 5c, respectively. At the presented stage, the flow field has already become rather complex but still exhibits considerable symmetry. The wave has passed the square cylinder causing a separation of flow with a subsequent generation of vortices both at the leading and trailing edges. Swept downstream by the flow, these vortices interact with reflected and diffracted shock waves thus generating new sets of weaker waves that follow the leading shock system. This leading front consists of the two wave segments that have been diffracted at the rear corners of the square cylinder, and a Mach stem that has emerged at a later instant during the intersection of the two diffracted shocks. The V-shaped slip lines behind the Mach stem hint at the location of the onset of Mach reflection. The color and the shade of gray, respectively, of the flow region immediately behind the Mach stem reveal that the onset of this irregular type of reflection leads to a stronger compression of the gas. This is also indicated in Fig. 5b by the appearance of the blue color in this zone indicating a positive gradient from left to right. Similarly, a region of increased density can be detected close to the top and bottom wall of the tube: here, the wave that has been reflected first from the obstacle and subsequently from the walls has caught up with the leading diffracted waves.

As a vortex induces both expansion and compression to the flow with respect to a certain direction, in the one-dimensionally working methods it will always be represented by two colors or shades of opposite sides of the spectrum. In the monochrome example of Fig. 5a the compression exceeds the sensitivity range thus obscuring a good deal of the flow field immediately behind the square cylinder. The corresponding color method can resolve this region showing clearly the extension of the two vortices. This is also true for the 2-D method, where vortices produce a color pattern being the inverse of the correlation diagram.

When the flow field gets more complex, black-and-white pictures may be hard to interpret. Highly turbulent regions may veil important flow patterns. Figure 6 shows the interaction of a shock wave reflected from the end wall with the boundary layer developed by the incident shock ($M_s \approx 3.85$ in CO_2, initial pressure $p_1 = 4$ kPa). In Fig. 6b, these boundary layers can clearly be identified as green and violet regions on the top and bottom walls (the different colors result from opposite gradient directions). Unlike the 2-D method which records all gradients in the flow field, the one-dimensionally working techniques cannot visualize these boundary layers which are characterized by a gradient parallel to the cutoff edges. In Fig. 6b, all features of the reflected shock bifurcation pattern can clearly be recognized, see e.g. Mark (1958) for details: the precursing 'foot' of the interaction, the triple point and the reflected second oblique shock that terminates in the growing boundary layer recirculation bubble, and the

Fig.5a-c. Interaction of a shock wave with a square cylinder. M_s: shock Mach number in N_2 initial pressure $p_1 = 100$ kPa a black-and-white method, $M_s = 1.25$ b 2-D method with calibration picture, $M_s = 1.25$ c 1-D method with calibration picture, $M_s = 1.24$

Fig.6a-c. Shock bifurcation due to interaction of the shock reflected from the end wall with the boundary layer. M_s: Shock Mach number of incident shock in CO_2, initial pressure $p_1 = 4$ kPa, a black-and-white method, $M_s = 3.81$, b 2-D method, $M_s = 3.85$, c 1-D method with calibration picture, $M_s = 3.87$.

Fig.7a-c. Interaction of a shock wave with a square cylinder. M_s: shock Mach number in CO_2, initial pressure $p_1 = 4$ kPa, a 2-D method, $M_s = 2.47$, b 2-D darkfield method, $M_s = 2.49$, c 1-D method, $M_s = 2.52$.

Fig.8a-c. Applications of the 2-D method. a Interaction of a shock wave with a vertical edge. Shock Mach number $M_s = 1.32$ in N_2, initial pressure $p_1 = 100$ kPa, b Interaction of a shock wave with a ramp. Shock Mach number $M_s = 2.25$ in N_2, initial pressure $p_1 = 4$ kPa, c Flat plate with rearward facing step in hypersonic flow. Angle of attack $\alpha = 15°$, free stream Mach number $M_\infty = 7.9$, free stream Reynolds number per meter $Re_\infty = 3.5 \times 10^6$ m^{-1}.

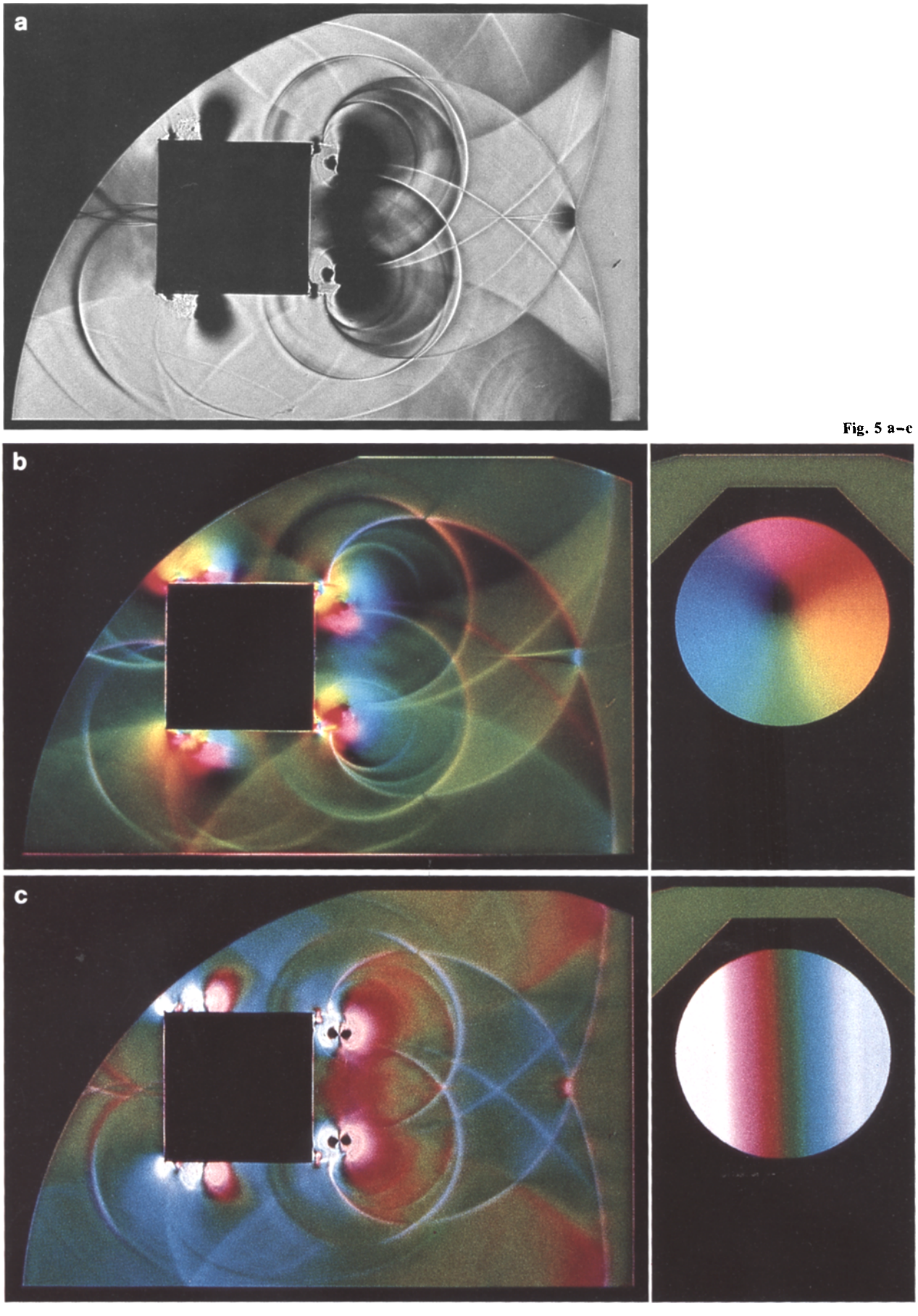

Fig. 5 a–c

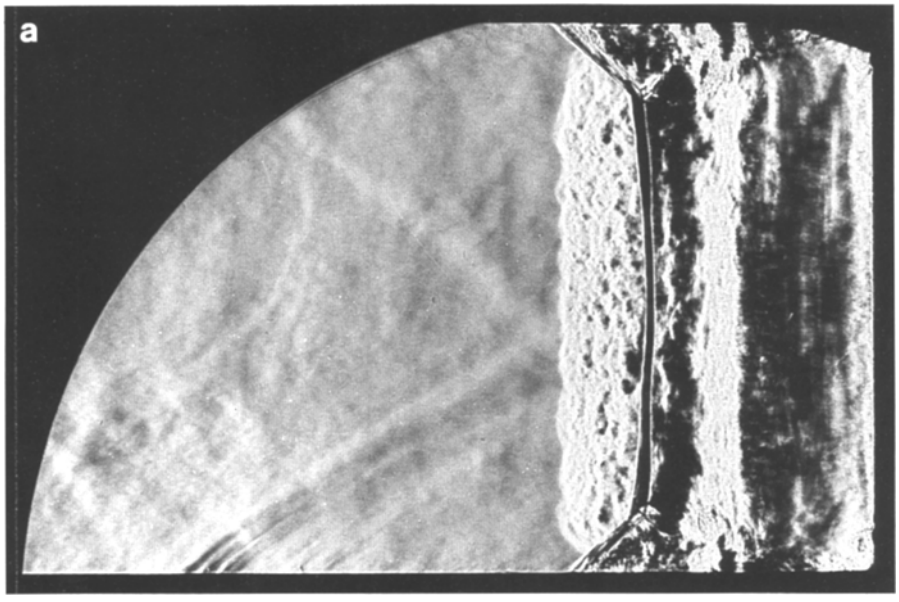

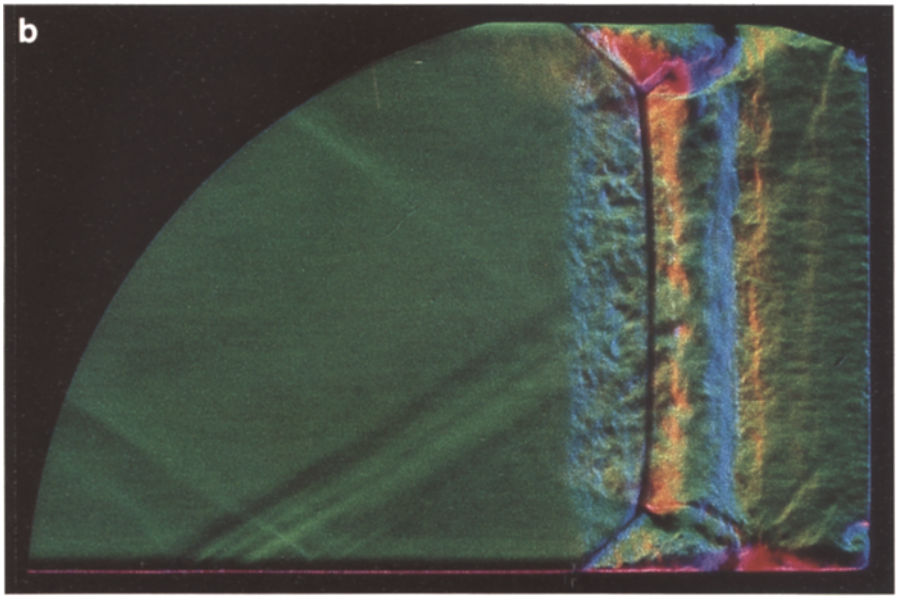

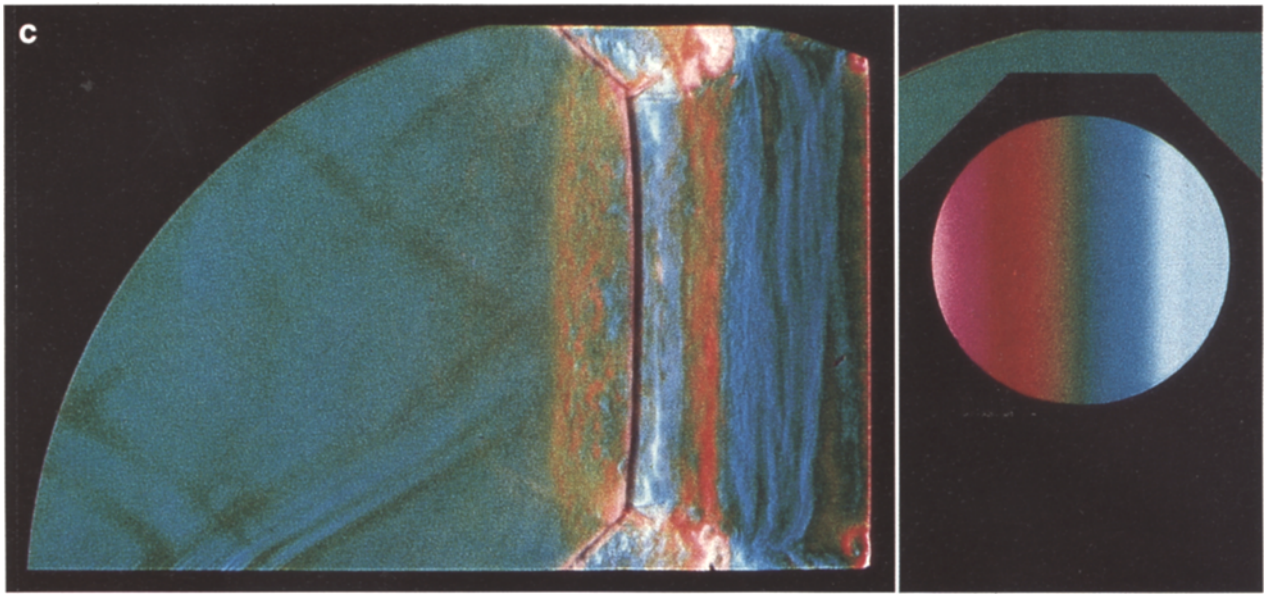

Fig. 6 a–c

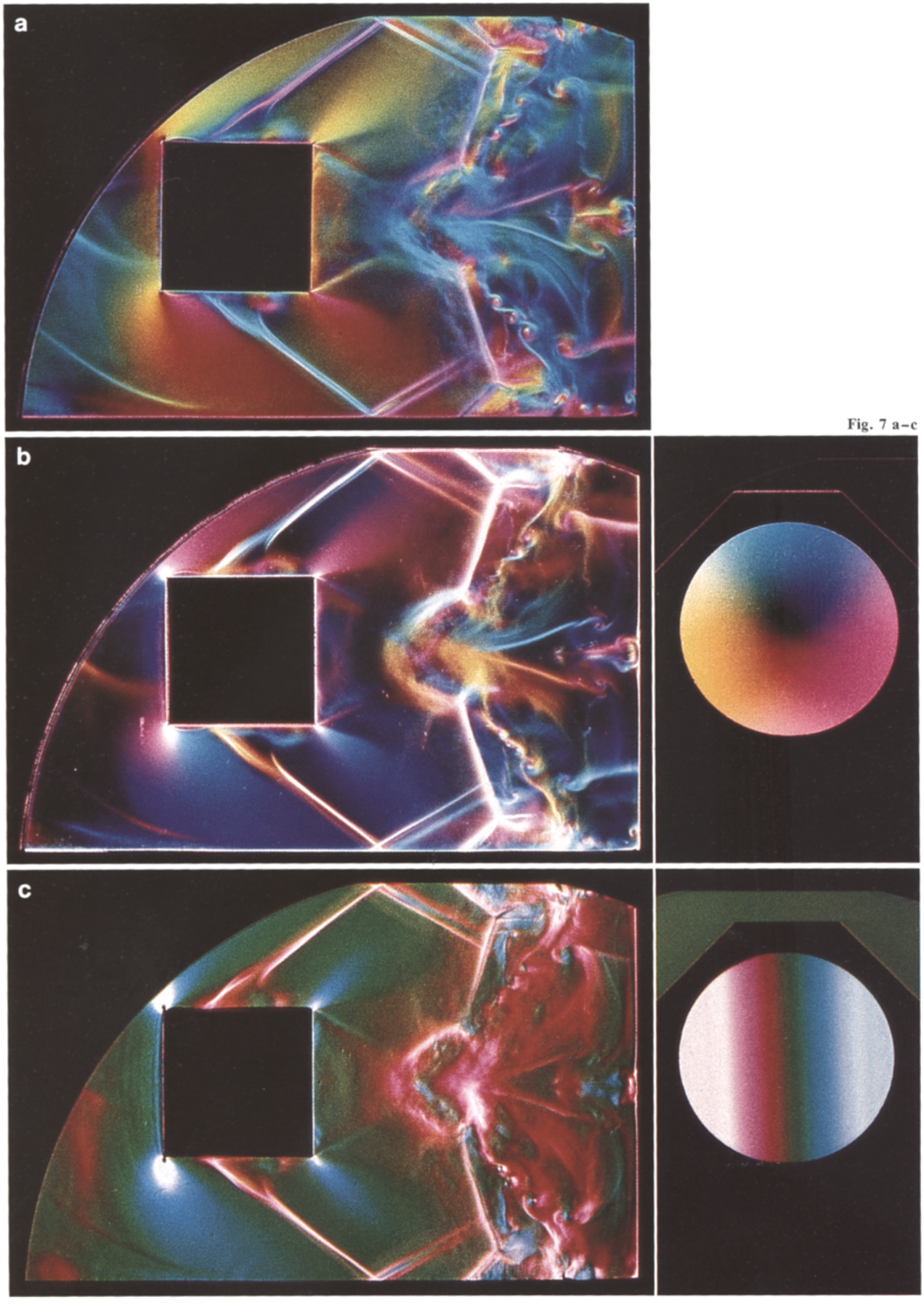

Fig. 7 a–c

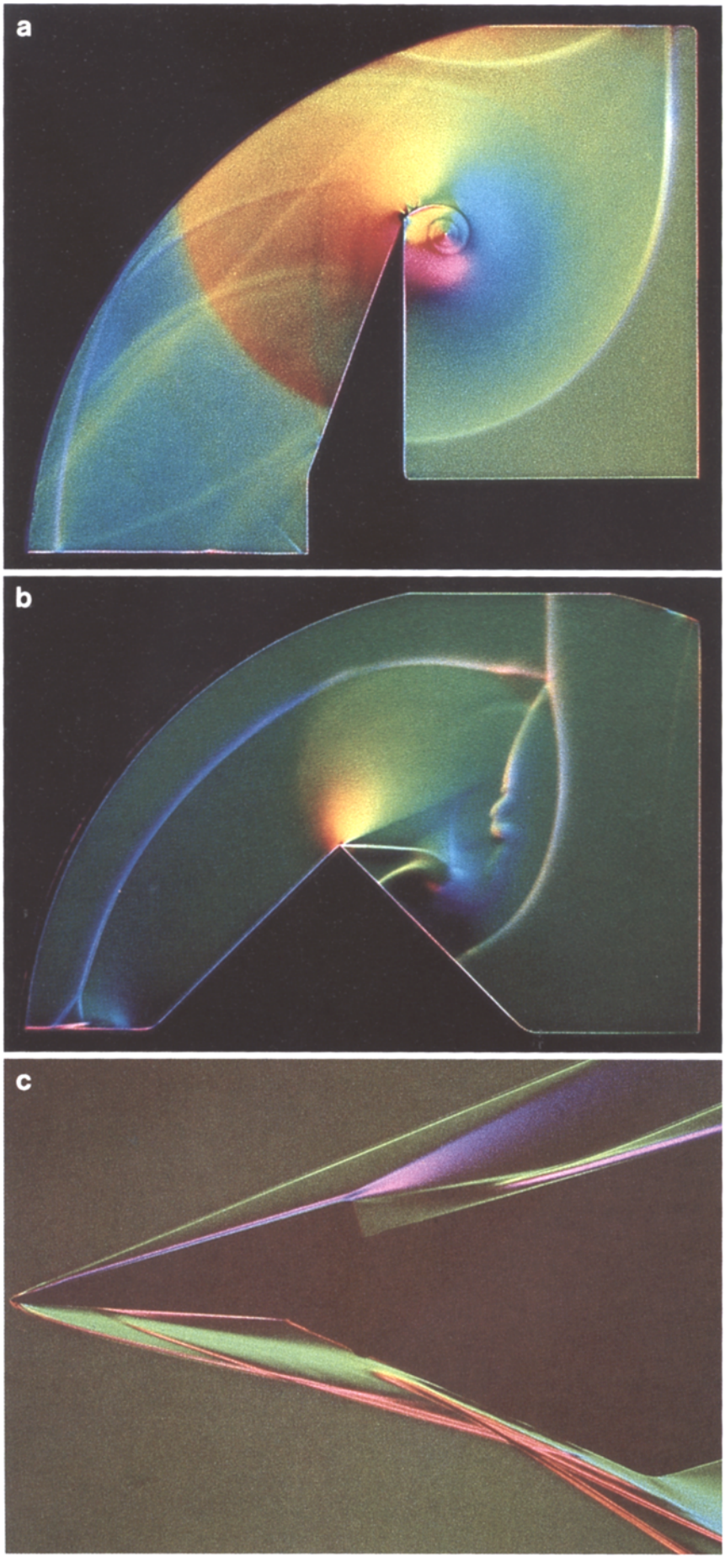

Fig. 8 a–c

slip stream separating the main part of the flow that has passed through the single normal shock from the part that was compressed twice by the two oblique shocks. This slip stream rolls up to form a vortex close to the end wall, which is hardly detectable in Fig. 6a, while it can be clearly identified in the color pictures. Moreover, the region of reversed flow headed for the channel walls, which is responsible for a significant pressure rise in corresponding measurements, can easily be distinguished from the rest on these pictures while its location might only be guessed for the monochrome case. The Mach lines, emerging from small disturbances on the shock tube floor and generated in the flow behind the incident shock, are clearly visible in all three pictures revealing a comparable sensitivity.

The flow field shown in Fig. 7 combines the features of the phenomena previously discussed: a shock wave ($M_s \approx 2.49$ in CO_2, initial pressure $p_1 = 4$ kPa) has passed a square cylinder creating a set of 'standing' lambda-shaped waves on the top and the bottom of the obstacle. Two Prandtl-Meyer fans (the flow behind the shock is supersonic now) at the rear corners expand the flow that forms a typical narrowing wake behind the square cylinder. The leading shock system, which again consists of diffracted parts and a Mach stem, has reflected from the end wall and begun to interact with the wake. On the top and bottom wall, bifurcation patterns can be recognized. As the shock front consisted of different parts its reflection has lead to a number of rolling up slip stream sheets. In the region of direct interaction with the wake the shock bifurcates again. In a similar fashion to boundary layer interaction, this might be explained by assuming that the stagnation pressure of the energy deficient fluid in the wake is lower than the pressure behind the reflected shock.

The main features and dominant structures are clearly seen in the darkfield picture of Fig. 7b (actually, the shock bifurcation in the wake is more obvious here than in the other pictures), smaller details (e.g. of the wake), however, are more difficult to perceive. Yet, this method might be useful to 'filter' a flow field with respect to strength and significance of the individual patterns. Figure 7c gives additional information about the magnitude of compression ($\Rightarrow$ red) and expansion zones ($\Rightarrow$ bluish white).

The examples given in Fig. 8 illustrate once more the diagnostic potential of color methods. It should be noted that the vortex spiral as well as the system of lambda-shocks close to the vertical edge in Fig. 8a can hardly be made visible with black-and-white schlieren methods. Comparable results have so far only been reached by corresponding shadowgraphs (Duff 1948).

When the wave has to pass a ramp, features typical of both reflection and diffraction processes can be observed. At the rising flank of the ramp a certain reflection pattern is set up which is determined by shock Mach number, test gas and ramp angle. In the given example of Fig. 8b ($M_s = 2.25$ in N_2; initial pressure $p_1 = 4$ kPa; ramp angle $\alpha = 45°$) a complex Mach reflection has occurred causing the appearance of the Mach stem, the kinked reflected shock and the curling-up slip stream. When the corner of the ramp is reached, this reflection pattern propagates further into the widening channel. While the wave system close to the triple point seems to be only mildly affected by this sudden area change the leading Mach stem is diffracted at the corner creating a flow pattern largely similar to the one observed for a simple 90° diffraction. The expansion zone (which due to the presence of the reflected shock is not a simple Prandtl-Meyer fan) is followed by a roughly triangular region where flow properties should be constant (the direction of that flow is almost horizontal). The boundaries of this region are the last characteristic of the expansion fan (top side), a second S-shaped shock (right hand side) and the slip stream (bottom side). The slip stream eventually rolls up to form a vortex, which also terminates the S-shock. This vortex induces a flow heading up the rear wall of the ramp, which is subsequently stopped by a third shock almost perpendicular to the ramp surface. Hardly detectable at this stage, the diffracted shock has developed another Mach reflection on its way down the rear side of the ramp. A more elaborate discussion of the basic shock wave interaction problems encountered here is provided e.g. by Bazhenova et al. (1984).

The flow pattern established in a hypersonic stream around a flat plate with a rearward-facing step is presented in Fig. 8c (free stream Mach number $M_\infty = 7.9$; height of step $h = 6$ mm; angle of attack $\alpha = 15°$). Once compressed by the leading shock at the tip of the wedge the flow follows the plate surface while the boundary layer obviously thickens. A large expansion fan at the corner turns the flow towards the lower part of the plate - the associated separation leads to the so-called lip-shock terminating this region of expanded flow. Finally, the flow meets the lower plate where the re-attachment shock is formed. Again, a thick boundary layer develops on the surface of the plate. These features have been investigated in greater detail e.g. by Gai et al. (1987). In this example, the different colors help to determine the nature of the observed flow pattern (note that the correlation diagram of Fig. 3b has to be inverted): for instance, the green hue representing an increase of density in top-to-bottom direction clearly identifies the lower boundary of the expanded flow region as the lip-shock.

8. Conclusions

The given outline of the color methods based on the dissection technique has exposed both limitations and possibilities of these configurations. It could be shown that the performance of corresponding black-and-white systems can be reached and – for certain aspects – exceeded. Although ultra-high sensitivities will remain the domain of black-and-white methods, color techniques are attractive because of their enlarged sensitivity range, not to mention the aesthetic value of these pictures (which should not be underestimated). The two-dimensional method moreover allows one to record all gradients of a flow field in a single picture, which in some cases may

be the only way to understand a complex flow. Special attention should be given to the possibility of tailoring a mask according to a certain problem to be investigated. New details invisible so far for more coarsely working methods may be recognized this way.

The main limiting factor at least for short duration applications appears to be the light source. Some improvements and optimizations in this field may even enhance the performance of the color techniques.

It should be made clear that it is not the purpose of this paper to label the conventional black-and-white methods as obsolete and ready to be replaced - yet, it should have become obvious that color offers new possibilities of insight into a large number of gas dynamic problems.

Acknowledgements. We would like to express our thanks to M. Kroll for her careful and fine work concerning the processing and reproduction of the color pictures.

References

Bazhenova TV, Gvozdeva LG, Nettleton MA (1984) Unsteady interactions of shock waves. Prog Aerospace Sci 21:249

Ben-Dor G, Takayama K, Needham CE (1987) The thermal nature of the triple point of a Mach reflection. Phys Fluids 30:1287

Ciezki H (1984) Entwicklung eines Farbschlierenverfahrens unter besonderer Berücksichtigung des Einsatzes an einem Stosswellenrohr. Diploma Thesis at the Lehrstuhl für Allgemeine Mechanik, RWTH Aachen

Cords PH (1968) A high resolution, high sensitivity color schlieren method. SPIE J 6:85

Duff RE (1948) In: van Dyke M (ed) An album of fluid motion. The Parabolic Press, Stanford, Cal. pp 145

Gai SL, Reynolds NT, Baird JP (1987) Heat transfer and interferometric study of the flow over a rearward facing step in hypersonic high enthalpy stream. In: Grönig H (ed) Proc 16th Int Symp on Shock Tubes and Waves, Aachen, VCH Weinheim pp 153

Hermann D (1987) Umströmungs - und Wärmeübertragungsvorgänge an einem Kreiszylinder im Stosswellenrohr. Dissertation, RWTH Aachen, VDI rept 143:17

Hibberd MF (1987) Color schlieren of eddies in a free shear flow. In: Veret C (ed) Flow visualization IV. Hemisphere Publishing Corp, New York pp 415

Holder DW, North RJ (1952) A schlieren apparatus giving an image in color. Nature 15:466

Holder DW, North RJ (1956) Optical methods for examining the flow in high-speed wind tunnel, Part I: schlieren methods. AGARDograph 23

Kleine H, Gvozdeva LG, Grönig H (1990) Visualization of transition phenomena by means of a 2-D color schlieren method. Proc 9th Int Mach Reflection Symp, Ernst-Mach-Institut, Freiburg, FRG

Mark H (1958) The interaction of a reflected shock wave with the boundary layer in a shock tube. NACA TM 1418

Miyashiro S, Grönig H (1985) Low-jitter reliable nanosecond spark source for optical short-duration measurements. Exp Fluids 3:71

North RJ (1954) A color schlieren system using multicolor filters of simple construction. NPL Aero Note 266

Oertel H, Oertel H jr (1989) Strömungsmesstechnik. G. Braun, Karlsruhe pp 279

Olivier H, Grönig H (1988) Untersuchung von Hyperschallströmungen im Aachener Stosswellenkanal. DGLR Jahrbuch I:354

Rheinberg J (1896) On an addition to the methods of microscopical research, by a new way of optically producing color-contrast between an object and its background, or between definite parts of the object itself. J Royal Microscop Soc pp 373

Schardin H (1942) Die Schlierenverfahren und ihre Anwendungen. Erg der exakt Naturwiss 20:303 (translated in: NASA TTF-12731 1970)

Settles GS (1970) A direction-indicating color schlieren system. AIAA J 12:2282

Settles GS (1982) Color schlieren optics - A review of techniques and applications. In: Merzkirch W (ed) Flow visualization II. Hemisphere Publishing Corp, New York pp 749

Settles GS (1983) Large-field color schlieren visualization of transient fluid phenomena. Bul Am Phys Soc 9:1404

Settles GS, Kuhns JW (1984) Visualization of airflow and convection phenomena about the human body. Bul Am Phys Soc 9:1515

Settles GS (1985) Color-coding schlieren techniques for the optical study of heat and fluid flow. Int J Heat and Fluid Flow 6:3

Stong CL (ed) (1971) Schlieren photography is used to study the flow around small objects. Scientific American 5:118

Vandiver JK, Edgerton HE (1974) Color schlieren photography of short duration transient events. Proc 11th Int Congr on High Speed Photog, London pp 398

Wolter H (1950) Zweidimensionale Farbschlierenverfahren. Annalen der Physik 6 Folge Band 8 Heft 1-2:1

Wuest W (1967) Sichtbarmachung von Strömungen, IV. Das Schlierenverfahren. Archiv für Techn Messen 5:81

This article was processed using Springer-Verlag TEX Shock Waves macro package 1990.